THE GLOBAL CONTRACTION OF MERCURY.

Paul K. Byrne[1,2], Christian Klimczak[1], A. M. Celâl Şengör[3], Sean C. Solomon[1,4], Thomas R. Watters[5], and Steven A. Hauck, II[6], [1]Department of Terrestrial Magnetism, Carnegie Institution of Washington, Washington, DC 20015, USA (pbyrne@carnegiescience.edu); [2]Lunar and Planetary Institute, Universities Space Research Association, Houston, TX 77058, USA; [3]Department of Geology, Istanbul Technical University, Istanbul, Turkey; [4]Lamont-Doherty Earth Observatory, Columbia University, Palisades, NY 10964, USA; [5]Center for Earth and Planetary Studies, National Air and Space Museum, Smithsonian Institution, Washington, D.C. 20560, USA; [6]Department of Earth, Environmental, and Planetary Sciences, Case Western Reserve University, Cleveland, Ohio 44106, USA.

- **Almost 6,000 shortening structures mapped, classified as one of four types**
- **In places, contraction is localized into long fold-and-thrust belts**
- **Mercury has contracted by as much as 7 km, far more than the 0.8–3 km previously reported**

Background. Mercury is replete with tectonic structures interpreted to be the result of planetary cooling and contraction [1], but the number and distribution of these structures, and their relation to topography, have not been well understood. Moreover, previous estimates of the amount of global contraction inferred from spacecraft images (0.8–3 km) [1–4] were far less than predicted by models of interior thermal evolution (~5–10 km) [5,6]. Here we use orbital observations acquired by the MErcury Surface, Space ENvironment, GEochemistry, and Ranging (MESSENGER) spacecraft to develop a synthesis of the global contraction of the innermost planet, and we show that Mercury has experienced much greater contraction than has previously been recognized.

Shortening Structure Classes. Two primary tectonic expressions of crustal shortening have been observed on Mercury: wrinkle ridges and lobate scarps [1]. Wrinkle ridges are typically broad, low-relief arches, often superposed by a narrow ridge. Lobate scarps are characterized by a steeply sloping scarp face and a gently sloping back limb, and are generally larger and presumably accommodated more shortening than wrinkle ridges. (A less common form of scarp is known as a high-relief ridge.)

We identify 5,934 ridges and scarps that we attribute to global contraction; individual fault-related features range from ~9 to 900 km in length, and their cumulative length is 4.16×10^8 m. In contrast to previous studies that separated wrinkle ridges, lobate scarps, and high-relief ridges [e.g., 3], here we classify the majority of mapped shortening structures by the primary terrain type—smooth plains [7] or cratered plains (a term we use here to refer to terrain that includes both the intercrater plains and heavily cratered terrain units described from Mariner 10 images [8])—in which they occur. Under this approach, most mapped landforms are classified as "smooth plains structures" or "cratered plains structures"; the remaining structures are either spatially associated with impact craters and so are termed "crater-related," or border areas of high-standing terrain and are catalogued as "high-terrain bounding" (**Fig. 1**).

Regional-scale crustal deformation. There is no clear evidence of a globally coherent lithospheric fracture pattern that survived the Late Heavy Bombardment, such as that predicted to have been influenced by tidal despinning [9]. Nonetheless, there is evidence of systematic regional-scale deformation on Mercury, for in places, groups of ridges and scarps form laterally contiguous, narrow bands of considerable length.

One such system extends for some 1,700 km (over 40° of arc) across Mercury's northern hemisphere and includes Victoria and Endeavour Rupēs and Antoniadi Dorsum. Many of its constituent landforms are cratered plains structures, but those that comprise its northern portion border an area of high-standing terrain to the west and show evidence of displacement (i.e., vergence) eastward onto the adjacent smooth plains. This sense of vergence is echoed by the other high-terrain bounding structures along its length. An even longer system, 1,800 km long, extends from 19°N, 55°E to 23°S, 61°E and also has a dominant (westward) vergence. We regard these systems as Mercury's equivalent of fold-and-thrust belts (FTBs) on Earth [10] and Venus [11].

Planetary radius change. From our global survey of mapped structures, we estimated the accumulated decrease in Mercury's radius accommodated by mapped structures using two methods. With the first, we summed the individual estimates of horizontal shortening across 216 structures intersected by eight great circles (shown on **Fig. 1**). For an assumed dip angle (θ) of 25°, 30°, and 35° for the thrust faults underlying each contractional landform, this method gives a mean change in planetary radius of 5.5 km, 4.4 km, and 3.7 km, respectively.

We also used those same 216 structures to define a scaling relation (γ) between maximum fault displacement (D_{max}) and fault length (L) for extrapolation to all mapped landforms, as used in previous studies [e.g., 4]. After subtracting the surface areas of Caloris and Rembrandt basins, whose interior structures were not

included in this analysis [cf. 12], we calculated radius change values of 7.1 km, 5.7 km, and 4.7 km for the same three values of θ as those above.

A portion of the strain accommodated by smooth plains structures may be due to load-induced flexure and subsidence. We therefore also estimated values of radial contraction with no smooth-plains structures included. When the surface area of smooth plains (~27% of the total planetary surface [7]) is excluded, together with that of the Caloris and Rembrandt interiors, the change in planetary radius for θ=25°, 30°, and 35° is 6.3 km, 5.1 km, and 4.2 km, respectively.

Concluding Remarks. Our finding that Mercury's radius has changed by up to a factor of seven greater than previous results resolves a nearly four-decades-old paradox: the history of heat production and loss and the accumulated global contraction are now consistent [5,6]. Our findings are crucial to thermal history models that will address the bulk silicate abundances of heat-producing elements, the question of whether the mantle is currently convecting [13], and the history of cooling and present-day structure of the large metallic core, the source of Mercury's internal magnetic field [5].

References. [1] Strom, R. G. et al. (1975) *JGR*, *80*, 2,478–2,507. [2] Watters, T. R. et al. (1998) *Geology*, *26*, 991–994. [3] Watters, T. R. et al. (2009) *Earth. Planet. Sci. Lett.*, *285*, 283–296. [4] Di Achille, G. et al. (2012) *Icarus*, *221*, 456–460. [5] Solomon, S. C. (1977) *Phys. Earth. Planet. Inter.*, *15*, 135–145. [6] Dombard, A. J. & Hauck, S. A., II (2008) *Icarus*, *198*, 274–276. [7] Denevi, B. W. et al. (2013) *JGR*, *118*, 891–907. [8] Trask, N. J. & Guest, J. E. (1975) *JGR*, *80*, 2,641–2,477. [9] Melosh, H. J. & Dzurisin, D. (1978) *Icarus*, *35*, 227–236. [10] Poblet, J. & Lisle, R. J. (2011) *Geol. Soc. Lond. Spec. Pub.*, *349*, 1–24. [11] Burke, K. C. et al. (1984) *LPS*, *15*, 104–105. [12] Byrne, P. K. et al. (2013) *LPS*, *44*, abstract 1,261. [13] Michel, N. C. et al. (2013) *JGR*, *117*, 1,033–1,044. [14] Becker, K. J. et al. (2012) *LPS*, *43*, abstract 2,654.

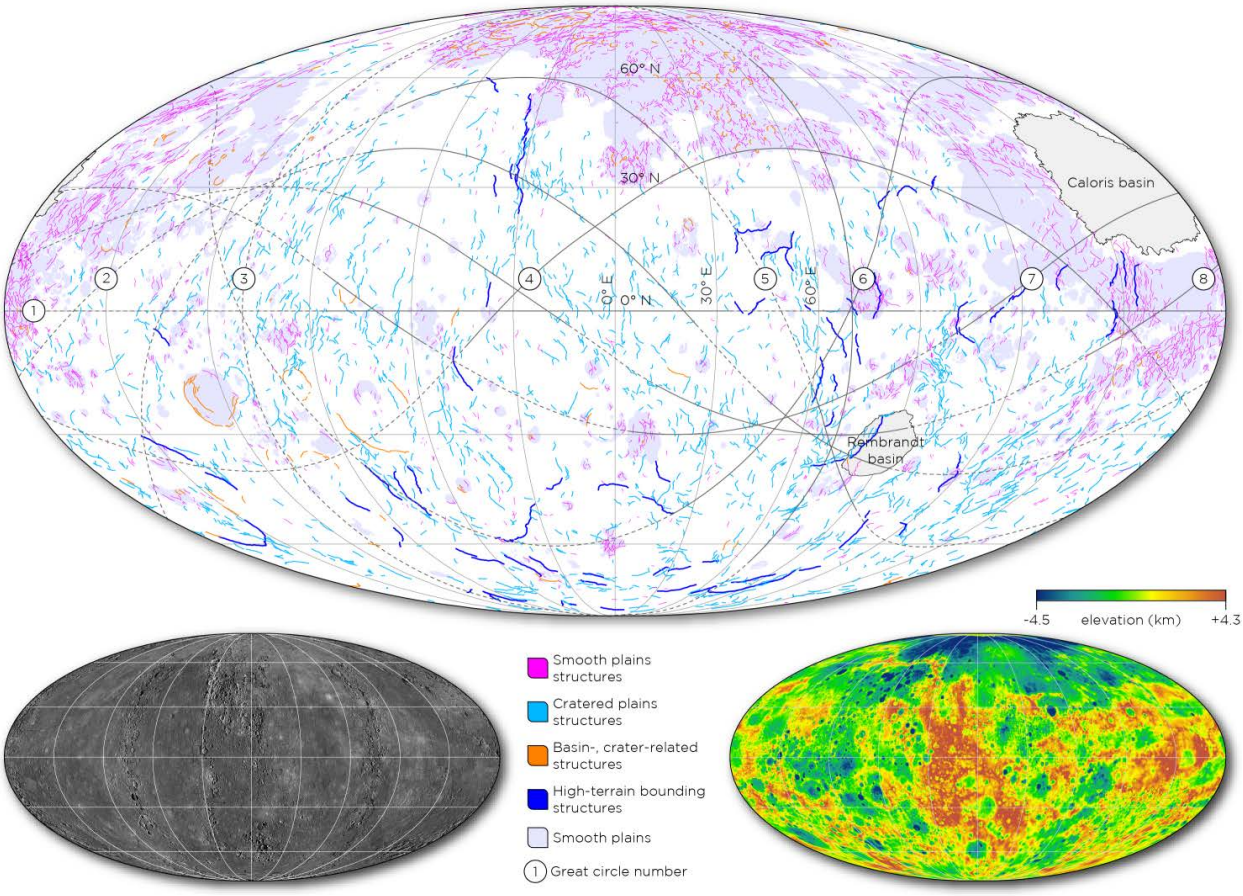

Fig. 1. Shortening structures on Mercury. The 5,934 classified thrust-fault-related landforms of this study; mapped smooth plains [7] are shown, as are the Caloris and Rembrandt basins. Measurements were taken along the unbroken portions of great circles 1–8. The global MDIS combined high-incidence-angle and monochrome base map (**bottom left**) and topography derived from the controlled MDIS wide-angle camera base map [14] (**bottom right**) used in this study are also shown. Each map is in a Mollweide projection centred at 0°E; the graticule is shown in 30° increments.